ACS Macro Letters

Letter

pubs.acs.org/macroletters

Experimental Studies on the Anisotropic Thermoelectric Properties of Conducting Polymer Films

Qingshuo Wei,* Masakazu Mukaida,* Kazuhiro Kirihara, and Takao Ishida

Nanosystem Research Institute, National Institute of Advanced Industrial Science and Technology, 1-2-1 Namiki, Tsukuba, Ibaraki 305-8564, Japan

Supporting Information

ABSTRACT: We reported general methods for studying the thermoelectric properties of a polymer film in both the in-plane and through-plane directions. The bench-mark PEDOT/PSS films have highly anisotropic carrier transport properties and thermal conductivity. The anisotropic carrier transport properties can be explained by the lamellar structure of the PEDOT/PSS films where the PEDOT nanocrystals could be isolated by the insulating PSS in the through-plane direction. The anisotropic thermal conductivity was mainly attributed to the lattice contribution from PSS because the polymer chain is oriented along the substrate.

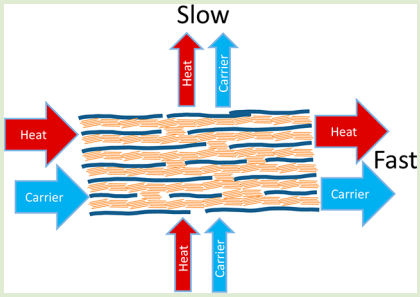

Organic electronics, such as organic light emitting diodes, organic solar cells, and organic thin film transistors, have attracted much attention in the past 20 years because of their low production costs, flexibility, and potential use in large-area products.[1] Thanks to the efforts in the development of organic conducting materials, their physical and chemical properties can now be tuned over a large range. This makes organic semiconductors suitable for many new applications that can utilize the advantages of organic materials. A recent example is their use in thermoelectric devices, which directly convert heat energy to electricity.[2−5] The Seebeck coefficient, S, the electrical conductivity, σ, and the thermal conductivity, κ (or the thermal diffusivity, α) are the most important parameters for evaluating thermoelectric materials. Several pioneering groups have reported devices containing organic semiconductors with excellent thermoelectric performance,[6−17] and we have demonstrated that organic thermoelectric devices can be used to power practical devices.[18] This shows that the performance of organic thermoelectrics could approach that of their inorganic counterparts.

For most organic semiconductors, it is difficult to make a dense block on a millimeter scale. Therefore, a common approach to characterizing organic thermoelectric materials is making a thin film and studying the in-plane electrical conductivity, in-plane Seebeck coefficient, and through-plane thermal conductivity. It is important to note that organic semiconductors have a preferred molecular orientation during film formation, which could produce an anisotropic film. Anisotropic films should show anisotropic thermoelectric properties; however, there are few studies on the anisotropic thermoelectric properties of organic semiconductors. Specifically, measuring the through-plane, four-probe electrical conductivity, through-plane Seebeck coefficient, and in-plane thermal conductivity is difficult. Rapid, reliable measurements of the thermoelectric properties of organic films in both directions are critically important for understanding the thermal transport and carrier transport in organic semiconductors further and for improving the performance of organic thermoelectric materials. Furthermore, the thermoelectric properties in both directions also affect thermoelectric device design. The performance of typical π-type thermoelectric devices is determined by the through-plane thermoelectric properties, whereas that of stacked thermoelectric devices is determined by the in-plane thermoelectric properties. In this paper, we report general approaches for studying the thermoelectric properties in both directions by using the benchmark conducting polymer poly(3,4-ethylenedioxythiophene)/poly(styrenesulfonate) (PEDOT/PSS). Temperature-dependent studies provide further information for understanding and improving the thermoelectric properties of organic materials through molecular design.

The through-plane conductivity of PEDOT/PSS has been studied by using two probe methods with a controlled electrode area.[12,13,19−21] To make rapid and reliable through-plane, four-probe conductivity measurements, we have designed a coaxial four-point probe based on previous studies by Lamson et al.[22] As shown in Figure 1a, the outer electrodes are used as the source probe (current probe) and the inner electrodes are used as the sense probe (voltage probe). All the probes are made of copper blocks plated with gold. The diameter of the outer source probe is 1 cm, and the diameter of the inner sense probe is 1 mm. The distance between the inner sense probe and the outer source probe is less than 500 μm (Figure 1b). To avoid shorting between sense probe and source probe, the sense probes were coated with a 30 μm thick layer of polyimide. The

Received: July 23, 2014
Accepted: September 3, 2014
Published: September 5, 2014

   dx.doi.org/10.1021/mz500446z | ACS Macro Lett. 2014, 3, 948−952

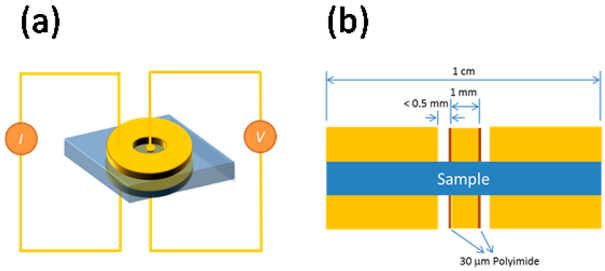

Figure 1. (a) Schematic representation and (b) cross-section of the through-plane, four-probe electrical conductivity measurement setup.

Ohmic contact between probes and the sample is necessary for reliable measurement. For the samples that have high in-plane conductivity, the errors are small due to the small voltage drop between source and sense probes. If there is a significant voltage drop between source and sense probes, the measurement could have a large error. Three different samples, including a stainless steel (SUS 304) block (7 mm thick), a highly ordered pyrolytic graphite (HOPG) substrate (1 mm thick), and a pyrolytic graphite sheet (PGS, 60 μm thick), were chosen to confirm the accuracy of our setup. These samples cover a large range of conductivity from 1 to 10^4 S/cm, and show both isotropic (SUS 304) and anisotropic (HOPG and PGS) conductivity. The SUS 304 block shows a through-plane conductivity of 1.6×10^4 S/cm (Table 1), which is comparable

Table 1. Summary of Electrical Conductivity Measured by Four-Probe Methods (S/cm) for Different Films

	SUS 304	HOPG	PGS	PEDOT
in-plane	1.3×10^4	430	4020	820
through-plane	1.6×10^4	3.4	18	36

with the in-plane value measured by using the four-point probe method (MCP-T610, Mitsubishi Chemical Corporation). The HOPG and PGS substrates show conductivities more than 2 orders of magnitude lower in the through-plane direction than in the in-plane direction, which is close to the theoretical calculation on graphite[23] and the reported experimental results.[24] This demonstrated the viability of the four-probe, through-plane conductivity measurements.

The through-plane electrical conductivity measurement was conducted on a free-standing PEDOT/PSS film with a thickness of about 100 μm. A 1 mm thick cross-linked poly(dimethylsiloxane) (PDMS; SILPOT 184, Toray) film was prepared in a 20 mL polystyrene bottle. PEDOT/PSS solution (10 mL) containing 3 wt % ethylene glycol was added to the bottle, and the mixture was heated on a hot plate at 70 °C for 2 days. After all the solvent was gone, the PEDOT/PSS film was easily detached from the PDMS substrate. The as-prepared free-standing PEDOT/PSS film was annealed at 150 °C for 30 min and then immersed in ethylene glycol for 30 min. This process was repeated three times to ensure the film had a highly ordered structure.[25] The film was around 100 μm thick, measured with a high-resolution digimatic measuring unit (VL-50-B, Mitsutoyo) with a measurement force of 1 N. The variation of the film thickness was less than 8%. The in-plane conductivity of the PEDOT/PSS films was measured as 820 S/cm (Table 1) by the four-point probe method, which was identical to the previously reported value, suggesting this thick film had an ordered structure similar to the thin films.[25]

However, the through-plane conductivity showed a lower value of 36 S/cm (the Ohmic contact between different probes is confirmed by current−voltage measurement, as shown in Supporting Information). It is important to point out that the through-plane conductivity measured by using a two-probe method (two outer source probes) was only 0.3 S/cm for the same sample, which was 2 orders of magnitude less than for the four-probe methods. This result is reasonable. For a 100 μm thick film with an electrode area of 0.8 cm^2, the resistance from the film was in the order of 10^{-4} Ω, which was very small compared with the contact resistance between metal and organic conducting materials. Therefore, the through-plane conductivity obtained by the four-probe method should be more reliable than the two-probe method measurements.

The anisotropic conductivity can be attributed to the morphology of the PEDOT/PSS films. Our previous studies have shown that highly conductive PEDOT/PSS films have a layered structure, and PSS may isolate the PEDOT nanocrystals in the through-plane direction.[25] This morphology may increase the mobility of the PEDOT/PSS film in the in-plane direction compared with the through-plane direction. The anisotropic conductivity can be further understood by taking temperature-dependent measurements in both directions, as discussed later.

It is difficult to obtain accurate measurements of the in-plane thermal conductivity of a thin film. The 3-omega method is ideal for studying the thermal conductivity of a thin film. By changing the size of the metal heater, both the in-plane and through-plane thermal conductivity can be explored. To make the in-plane thermal diffusivity measurements more straightforward, we prepared large-area, free-standing PEDOT/PSS films and studied them by using flash analysis methods. Figure 2a

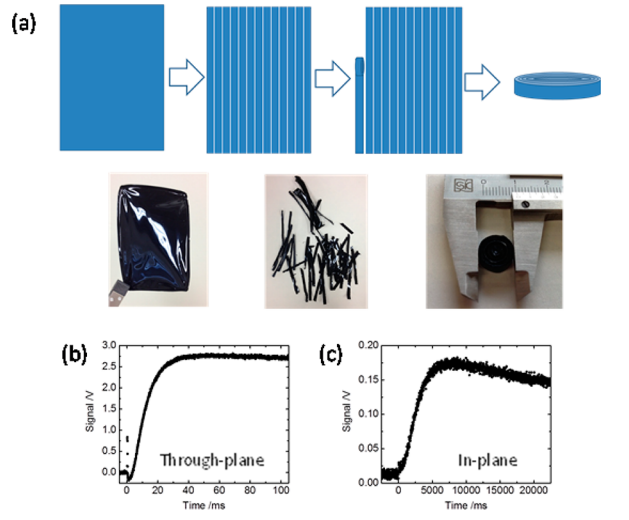

Figure 2. (a) Schematic and photographic images showing the sample preparation for the in-plane thermal diffusivity measurements. Temperature rise curves of the PEDOT/PSS film in the (b) through-plane and (c) in-plane directions.

shows the 15 × 20 cm free-standing film prepared following the previous method with PDMS as a substrate. The film was cut into 3.5 mm ribbons with a paper shredder, and then the ribbons were rolled into a disk with a diameter larger than 1 cm. Because the PEDOT/PSS films absorbed all the light from the xenon lamp, there was no need to use graphite spray. Figure 2b,c shows the temperature curves of the PEDOT/PSS film for

dx.doi.org/10.1021/mz500446z | ACS Macro Lett. 2014, 3, 948−952

the through-plane and in-plane directions. For the through-plane thermal diffusivity measurement, the half-rise time was 11.1 ms for a 95 μm thick film, which was much longer than the pulse width (0.3 ms) of the xenon lamp, suggesting that the measurements were reliable. We compared free-standing films of different thicknesses and found that films more than 30 μm thick gave a reliable, consistent thermal diffusivity value of 0.11 mm^2/s. Figure 2c shows that there was no light leak for the in-plane thermal diffusivity measurement, suggesting that the rolled PEDOT/PSS disk was very dense. The density, ρ, of the rolled block was about 1.1 g/cm^3, which was close to that of the free-standing samples (1.4 ± 0.2 g/cm^3). The in-plane direction gave a much higher thermal diffusivity value of 0.60 mm^2/s at 25 °C. The in-plane thermal diffusivity could contain larger errors compared with through-plane thermal diffusivity due to the uniformity of the PEDOT ribbons. The thickness variation of the rolled PEDOT/PSS disk was around 15%, which could introduce 30% errors on thermal diffusivity. We conducted differential scanning calorimetry measurements to determine the specific heat capacity, C_p, of the pure PEDOT/PSS, which was about 1.0 ± 0.2 J/g K at room temperature. The calculated thermal conductivity ($\kappa = \alpha \times C_p \times \rho$) in the through-plane direction was 0.15 W/m K, and the value of the in-plane direction was 0.84 W/m K. This suggests that the thermal conductivity of the ordered PEDOT/PSS films was highly anisotropic, similar to the electrical conductivity. The morphology of the organic films could easily be affected by the preparation process; therefore, the thermal conductivity of the organic thin film could vary over a large range depending on fabrication conditions.

To study the through-plane Seebeck coefficient of PEDOT/PSS, a homemade Seebeck coefficient measurement setup was designed. The key to accurate through-plane Seebeck coefficient measurements is obtaining a reliable temperature difference between the two surfaces. Figure 3a shows that the temperature on different sides of the film was controlled by two Peltier units (Ampere, UT40U100F). The temperature difference and the electromotive force were measured simultaneously by probing a pair of electrodes with a digital multimeter. The temperature difference was maintained at 0−10 °C, and more than 10 data points were measured for each temperature difference. To confirm this method can be used to measure the through-plane Seebeck coefficient, we used a 1 mm thick Ni substrate as a standard sample. The Ni plate gave a through-plane Seebeck coefficient of −17 μV/K at 25 °C (Figure 3b), which is close to the reported value.[26] This demonstrates the accuracy of the measurement method. Figure 3c shows the through-plane Seebeck coefficient measurements for the free-standing PEDOT/PSS film. The Seebeck coefficient in the through-plane direction was 15 μV/K at room temperature, which was close to that in the in-plane direction (17 μV/K). Compared with the Ni substrate, a temperature difference between the two sides of a thin PEDOT film was easy to achieve, suggesting low thermal conductivity in the through-plane direction. The calculated figure-of-merit at room temperature in the in-plane direction is around 8.4 × 10^{-3} and the through-plane direction is around 1.6 × 10^{-3}. Note that the calculated figure-of-merit by using in-plane electrical conductivity, in-plane Seebeck coefficient and through-plane thermal conductivity will give an overestimated value of 0.05. These results suggest that the performance of stacked thermoelectric modules should be better than the π-type modules. These measurements were conducted using pristine PEDOT/PSS films at a humidity of less than 55% at 25 °C, and the effects of water and other added solvents, such as ethylene glycol, were not considered here.[9,14] In contrast to the electrical and thermal conductivity, the Seebeck coefficient in the ordered PEDOT/PSS films was not highly anisotropic. This result is consistent with previous studies of inorganic semiconductors that have shown that highly anisotropic systems have almost isotropic Seebeck coefficients.[27,28]

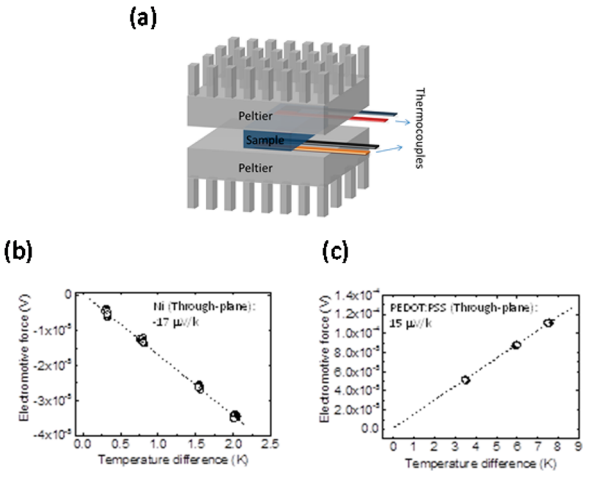

Figure 3. (a) Schematic representation of the through-plane Seebeck coefficient measurement setup. Seebeck coefficient measurements of (b) a Ni substrate and (c) a PEDOT/PSS film in the through-plane direction.

To understand the anisotropic thermoelectric properties of the PEDOT/PSS films further, we carried out temperature-dependent electrical conductivity, Seebeck coefficient, and thermal diffusivity measurements. Figure 4a shows that the in-plane electrical conductivity decreased with the temperature. However, the through-plane conductivity had a lower value and showed a positive temperature dependence, indicating hopping transport properties (the viability of the temperature-dependent, through-plane conductivity measurements was confirmed by using SUS304 and HOPG as standard samples, as shown in Supporting Information). The different carrier transport properties can also be observed from the temperature-dependent Seebeck coefficient measurements. Figure 4b shows that the in-plane Seebeck coefficient was almost independent of the temperature, whereas the through-plane Seebeck coefficient increased with the temperature, which is generally observed in thermoelectric materials with hopping transport mechanisms.[3] Using our current setup, there are difficulties in keeping the average sample temperature exactly the same in the in-plane and through-plane directions because of the different distances between the Peltier units during the in-plane and through-plane Seebeck coefficient measurements. The working temperature of the Peltier units in our setup was less than 125 °C, and the achievable sample temperature was less than 100 °C. The difference in the electrical conductivity and Seebeck coefficient for the through-plane and in-plane directions can be explained by the morphology of PEDOT/PSS films. As we reported previously, the PEDOT nanocrystal has an ordered layered structure in the film.[25] The well-packed PEDOT nanocrystal in the in-plane direction makes the carrier localization length larger than molecular spacing, which causes a high in-plane conductivity with a negative temperature dependence. For the through-plane direction, two possibilities

dx.doi.org/10.1021/mz500446z | ACS Macro Lett. 2014, 3, 948−952

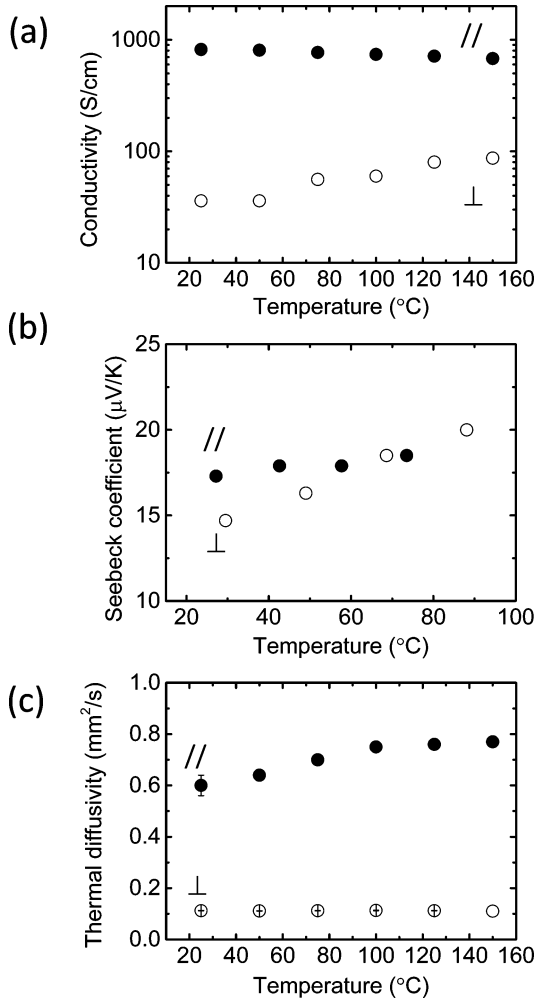

Figure 4. (a) Electrical conductivity, (b) Seebeck coefficient, and (c) thermal diffusivity of the PEDOT/PSS films in the in-plane (closed circles) and through-plane (open circles) directions, plotted as a function of temperature.

can be considered. First, the carrier mobility in the PEDOT nanocrystal is lower in the through-plane direction. Second, there are energy barriers between the PEDOT nanocrystals in the through-plane direction. The thiophene rings in PEDOT/PSS films show an average face-on packing, and the π-conjugated planes of the PEDOT crystal are more vertical with respect to the substrate.[25] Studies of organic thin film transistors have shown that the $\pi-\pi$ stacking direction generally has a high carrier mobility.[29,30] Therefore, the energy barriers between the PEDOT nanocrystals should play an important role in the through-plane carrier transport. The PEDOT/PSS films have a lamellar structure, and the PEDOT nanocrystals could be isolated by the insulating PSS, which could significantly reduce the overlap of the charge carrier wave functions.

The temperature-dependent thermal diffusivity is shown in Figure 4c. The through-plane thermal diffusivity is almost identical in this temperature range and the in-plane thermal diffusivity slightly increases with the temperature. Qualitative analysis of the temperature-dependent thermal diffusivity is difficult at this stage because the composition of PEDOT/PSS and the PSS chain conformation could be different at different temperatures. However, the trend in temperature-dependent thermal diffusivity for both directions is different from the temperature-dependent electrical conductivity (Figure 4a). Thus, the contribution to the thermal conductivity from the electronic part (charge carriers) should be smaller than that from the lattice part (phonons). In PEDOT/PSS, the amount of insulating dopant PSS is larger than conductive PEDOT. The anisotropic thermal conductivity should be related to the lattice contribution from PSS because the PSS chains in the film could be oriented along the in-plane direction. Heat is transported more efficiently through intrachain covalent bonding than through interchain van der Waals interactions.[31] The anisotropic thermal diffusivity and thermal conductivity are generally observed in solid polymers.[32] To improve the thermoelectric performance of PEDOT, one simple approach is to reduce the in-plane thermal conductivity by using a small-molecule dopant. In fact, PEDOT/tosylate, in which the polyanion (PSS) is replaced with small anions, showed almost isotropic thermal conductivity.[7]

In conclusion, we have developed general approaches for studying the thermoelectric properties of a polymer film in the in-plane and through-plane directions. We have shown that the bench-mark PEDOT/PSS films have anisotropic carrier transport properties and thermal conductivity. The anisotropic carrier transport properties can be explained by the lamellar structure of the PEDOT/PSS films, where the PEDOT nanocrystals could be isolated by the insulating PSS in the through-plane direction. The anisotropic thermal conductivity was attributed to the lattice contribution from PSS because the polymer chain is oriented along the substrate. The use of small-molecule dopants and controlling the crystal orientation could be effective strategies for optimizing the thermoelectric performance.

■ ASSOCIATED CONTENT

Ⓢ Supporting Information

Experimental details. This material is available free of charge via the Internet at http://pubs.acs.org.

■ AUTHOR INFORMATION

Corresponding Authors

*E-mail: qingshuo.wei@aist.go.jp.
*E-mail: mskz.mukaida@aist.go.jp.

Notes

The authors declare no competing financial interest.

■ ACKNOWLEDGMENTS

This work was supported in part by TherMAT, Future Pioneering Projects of the Ministry of Economy, Trade and Industry, Japan. This work was supported in part by a Grant-in-Aid for Research Activity Start-up 25888025 from MEXT, Japan.

■ REFERENCES

(1) Forrest, S. R.; Thompson, M. E. *Chem. Rev.* **2007**, *107*, 923−925.
(2) Snyder, G. J.; Toberer, E. S. *Nat. Mater.* **2008**, *7*, 105−114.
(3) Bubnova, O.; Crispin, X. *Energy Environ. Sci.* **2012**, *5*, 9345−9362.
(4) Poehler, T. O.; Katz, H. E. *Energy Environ. Sci.* **2012**, *5*, 8110−8115.
(5) Zhang, Q.; Sun, Y.; Xu, W.; Zhu, D. *Adv. Mater.* **2014**, DOI: 10.1002/adma.201305371.
(6) Zhang, B.; Sun, J.; Katz, H. E.; Fang, F.; Opila, R. L. *ACS Appl. Mater. Interfaces* **2010**, *2*, 3170−3178.

(7) Bubnova, O.; Khan, Z. U.; Malti, A.; Braun, S.; Fahlman, M.; Berggren, M.; Crispin, X. *Nat. Mater.* **2011**, *10*, 429−433.
(8) Sun, Y.; Sheng, P.; Di, C.; Jiao, F.; Xu, W.; Qiu, D.; Zhu, D. *Adv. Mater.* **2012**, *24*, 932−937.
(9) Kim, G. H.; Shao, L.; Zhang, K.; Pipe, K. P. *Nat. Mater.* **2013**, *12*, 719−723.
(10) Bubnova, O.; Khan, Z. U.; Wang, H.; Braun, S.; Evans, D. R.; Fabretto, M.; Hojati-Talemi, P.; Dagnelund, D.; Arlin, J.-B.; Geerts, Y. H.; Desbief, S.; Breiby, D. W.; Andreasen, J. W.; Lazzaroni, R.; Chen, W. M.; Zozoulenko, I.; Fahlman, M.; Murphy, P. J.; Berggren, M.; Crispin, X. *Nat. Mater.* **2014**, *13*, 190−194.
(11) Massonnet, N.; Carella, A.; Jaudouin, O.; Rannou, P.; Laval, G.; Celle, C.; Simonato, J.-P. *J. Mater. Chem. C* **2014**, *2*, 1278−1283.
(12) Russ, B.; Robb, M. J.; Brunetti, F. G.; Miller, P. L.; Perry, E. E.; Patel, S. N.; Ho, V.; Chang, W. B.; Urban, J. J.; Chabinyc, M. L.; Hawker, C. J.; Segalman, R. A. *Adv. Mater.* **2014**, *26*, 3473−3477.
(13) Schlitz, R. A.; Brunetti, F. G.; Glaudell, A. M.; Miller, P. L.; Brady, M. A.; Takacs, C. J.; Hawker, C. J.; Chabinyc, M. L. *Adv. Mater.* **2014**, *26*, 2825−2830.
(14) Wei, Q. S.; Mukaida, M.; Kirihara, K.; Naitoh, Y.; Ishida, T. *Appl. Phys. Express* **2014**, *7*, 031601.
(15) Hokazono, M.; Anno, H.; Toshima, N. *J. Electron. Mater.* **2014**, *43*, 2196−2201.
(16) Yoshida, A.; Toshima, N. *J. Electron. Mater.* **2014**, *43*, 1492−1497.
(17) Park, T.; Park, C.; Kim, B.; Shin, H.; Kim, E. *Energy Environ. Sci.* **2013**, *6*, 788−792.
(18) Wei, Q. S.; Mukaida, M.; Kirihara, K.; Naitoh, Y.; Ishida, T. *RSC Adv.* **2014**, *4*, 28802−28806.
(19) Nardes, A. M.; Kemerink, M.; Janssen, R. A. J.; Bastiaansen, J. A. M.; Kiggen, N. M. M.; Langeveld, B. M. W.; van Breemen, A. J. J. M.; de Kok, M. M. *Adv. Mater.* **2007**, *19*, 1196−1200.
(20) Na, S.-I.; Wang, G.; Kim, S.-S.; Kim, T.-W.; Oh, S.-H.; Yu, B.-K.; Lee, T.; Kim, D.-Y. *J. Mater. Chem.* **2009**, *19*, 9045−9053.
(21) Ando, K.; Watanabe, S.; Mooser, S.; Saitoh, E.; Sirringhaus, H. *Nat. Mater.* **2013**, *12*, 622−627.
(22) Lamson, M. A.; Gurrum, S. P.; Dunne, R. U.S. Patent 2009/0289648 A1, 2009.
(23) Slonczewski, J. C.; Weiss, P. R. *Phys. Rev.* **1958**, *109*, 272−279.
(24) Matsubara, K.; Sugihara, K.; Tsuzuku, T. *Phys. Rev. B* **1990**, *41*, 969−974.
(25) Wei, Q. S.; Mukaida, M.; Naitoh, Y.; Ishida, T. *Adv. Mater.* **2013**, *25*, 2831−2836.
(26) Burkov, A. T.; Heinrich, A.; Konstantinov, P. P.; Nakama, T.; Yagasaki, K. *Meas. Sci. Technol.* **2001**, *12*, 264.
(27) Yang, B.; Liu, W. L.; Liu, J. L.; Wang, K. L.; Chen, G. *Appl. Phys. Lett.* **2002**, *81*, 3588−3590.
(28) Shen, J. J.; Hu, L. P.; Zhu, T. J.; Zhao, X. B. *Appl. Phys. Lett.* **2011**, *99*, 124102.
(29) Sirringhaus, H.; Brown, P. J.; Friend, R. H.; Nielsen, M. M.; Bechgaard, K.; Langeveld-Voss, B. M. W.; Spiering, A. J. H.; Janssen, R. A. J.; Meijer, E. W.; Herwig, P.; de Leeuw, D. M. *Nature* **1999**, *401*, 685−688.
(30) Brédas, J. L.; Calbert, J. P.; da Silva Filho, D. A.; Cornil, J. *Proc. Natl. Acad. Sci. U.S.A.* **2002**, *99*, 5804−5809.
(31) Choy, C. L. *Polymer* **1977**, *18*, 984−1004.
(32) Kurabayashi, K. *Int. J. Thermophys.* **2001**, *22*, 277−288.